PROCEEDINGS OF SCIENCE

Factorization of the Drell-Yan q_T spectrum with massive quarks

Piotr Pietrulewicz
Theory Group, Deutsches Elektronen-Synchrotron (DESY), D-22607 Hamburg, Germany
E-mail: piotr.pietrulewicz@desy.de

Daniel Samitz*
University of Vienna, Faculty of Physics, Boltzmanngasse 5, A-1090 Wien, Austria
E-mail: daniel.samitz@univie.ac.at

Anne Spiering
School of Mathematics, Trinity College Dublin, College Green, Dublin 2, Ireland
E-mail: spiering@maths.tcd.ie

Frank J. Tackmann
Theory Group, Deutsches Elektronen-Synchrotron (DESY), D-22607 Hamburg, Germany
E-mail: frank.tackmann@desy.de

Exclusive differential spectra in color-singlet processes at hadron colliders are benchmark observables that have been studied to high precision in theory and experiment. We present an effective-theory framework utilizing soft-collinear effective theory to incorporate massive (bottom) quark effects into resummed differential distributions, accounting for both heavy-quark initiated primary contributions to the hard scattering process as well as secondary effects from gluons splitting into heavy-quark pairs. We discuss a variable flavor number scheme (VFNS) for the Drell-Yan process for the vector-boson transverse momentum q_T as an example of an exclusive observable. The theoretical description depends on the hierarchy between the hard, mass, and the q_T scale, ranging from the decoupling limit $q_T \ll m$ to the massless limit $m \ll q_T$. The phenomenologically relevant intermediate regime $m \sim q_T$ requires in particular quark-mass dependent beam and soft functions. We find that the rapidity divergences are different from the massless case and we discuss features of the resulting rapidity evolution. Our results will allow for a detailed investigation of quark-mass effects in the ratio of W and Z boson spectra at small q_T, which is important for the precision measurement of the W-boson mass at the LHC.

13th International Symposium on Radiative Corrections (Applications of Quantum Field Theory to Phenomenology)
25-29 September, 2017
St. Gilgen, Austria
Preprint: DESY 18-012

*Speaker.

PoS(RADCOR2017)053

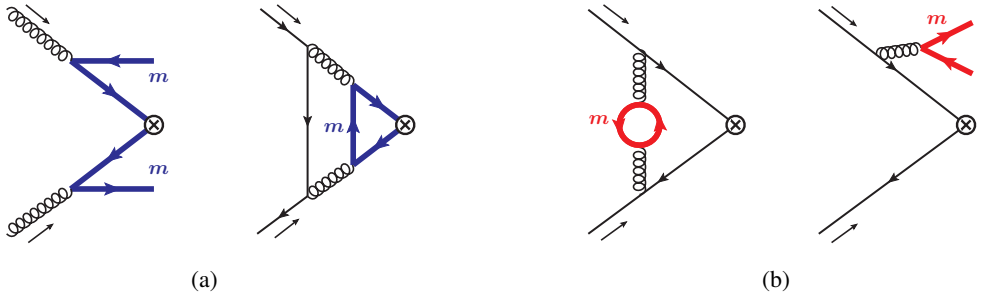

Figure 1: Primary (a) and secondary (b) heavy-quark mass effects for Z-boson production.

1. Factorization of quark mass effects for the q_T spectrum

1.1 Factorization for massless quarks

Before discussing the massive quark corrections, we first briefly summarize the EFT setup and factorization for $q_T \ll Q$ for massless quarks. Within this framework the factorized differential cross section with n_f massless quarks reads

$$\begin{aligned}\frac{\mathrm{d}\sigma}{\mathrm{d}q_T^2\,\mathrm{d}Q^2\,\mathrm{d}Y} = \sum_{i,j\in\{q,\bar{q}\}} H_{ij}^{(n_f)}(Q,\mu) \int \mathrm{d}^2 p_{Ta}\,\mathrm{d}^2 p_{Tb}\,\mathrm{d}^2 p_{Ts}\,\delta(q_T^2 - |\vec{p}_{Ta}+\vec{p}_{Tb}+\vec{p}_{Ts}|^2) \\ \times B_i^{(n_f)}\Big(\vec{p}_{Ta}, x_a, \mu, \frac{\nu}{\omega_a}\Big) B_j^{(n_f)}\Big(\vec{p}_{Tb}, x_b, \mu, \frac{\nu}{\omega_b}\Big) S^{(n_f)}(\vec{p}_{Ts}, \mu, \nu) \Big[1 + \mathscr{O}\Big(\frac{q_T}{Q}\Big)\Big],\end{aligned} \tag{1.1}$$

where

$$\omega_a = Qe^Y\,, \quad \omega_b = Qe^{-Y}\,, \quad x_{a,b} = \frac{\omega_{a,b}}{E_{\mathrm{cm}}}\,, \tag{1.2}$$

with Y denoting the rapidity of the Z-boson.

In eq. (1.1), the superscript (n_f) on all functions indicates that the associated EFT operators and the strong coupling constant in these functions are renormalized with n_f active quark flavors. The logarithms of q_T/Q are resummed by evaluating all functions at their characteristic renormalization scales and evolving them to common final scales μ and ν, where ν is the rapidity scale (see below).

H_{ij} denotes the process-dependent hard function. It encodes the tree-level result and hard virtual corrections of the partonic process at the scale $\mu \sim Q$. The soft function S describes the wide-angle soft radiation at the invariant mass and rapidity scale $\mu \sim \nu \sim q_T$. Following refs. [1, 2, 3], the renormalized transverse-momentum dependent (TMD) beam functions B_i, which are essentially equivalent to TMDPDFs, can be matched onto PDFs as

$$\begin{aligned}B_i^{(n_f)}\Big(\vec{p}_T, x, \mu, \frac{\nu}{\omega}\Big) &= \sum_k \int_x^1 \frac{\mathrm{d}z}{z}\, \mathscr{I}_{ik}^{(n_f)}\Big(\vec{p}_T, z, \mu, \frac{\nu}{\omega}\Big) f_k^{(n_f)}\Big(\frac{x}{z}, \mu\Big)\Big[1 + \mathscr{O}\Big(\frac{\Lambda_{\mathrm{QCD}}^2}{|\vec{p}_T|^2}\Big)\Big] \\ &\equiv \sum_k \mathscr{I}_{ik}^{(n_f)}(\vec{p}_T, x, \mu, \frac{\nu}{\omega}) \otimes_x f_k^{(n_f)}(x,\mu)\,,\end{aligned} \tag{1.3}$$

where the perturbative matching coefficients $\mathscr{I}_{ik}$ describe the collinear initial-state radiation at the invariant mass scale $\mu \sim q_T$ and rapidity scale $\nu \sim Q$, and the nonperturbative parton distribution functions (PDFs) are denoted by f_k. The matching coefficients $\mathscr{I}_{ik}$ and the soft function are process-independent and have been computed to $\mathscr{O}(\alpha_s^2)$ in refs. [4, 5, 6, 7] allowing for a full NNLL′ analysis of Drell-Yan for massless quarks.

The soft and collinear modes are only separated in rapidity leading to the emergence of rapidity divergences and associated rapidity logarithms. The traditional approach for their resummation in QCD relies on the work by Collins, Soper, and Sterman [8, 9, 10]. In SCET the factorization and resummation were devised in refs. [11, 12, 13, 14]. Here we use the rapidity renormalization approach of refs. [12, 13], where the rapidity divergences are regularized by a symmetric regulator and are renormalized by appropriate counterterms (by a $\overline{\text{MS}}$-type subtraction). The rapidity logarithms are then resummed by solving the associated rapidity renormalization group equations (see sec. 2).

1.2 Factorization with massive quarks

For Z-boson production at NNLL′, primary effects contribute via $\mathscr{O}(\alpha_s) \times \mathscr{O}(\alpha_s)$ heavy-quark initiated contributions, illustrated in fig. 1(a). Secondary effects contribute as $\mathscr{O}(\alpha_s^2)$ corrections to light-quark initiated hard interactions, illustrated in fig. 1(b). Due to the strong CKM suppression primary m_b-effects do not play any significant role for W-production, which represents a key difference to Z-boson production.

Here we do not discuss the factorization in the hierarchy $q_T \ll m \sim Q$, because it is not of phenomenological interest. For further details on the different factorization theorems for the different hierarchies as well as the one and two-loop results for the massive quark contributions to the beam and soft functions we refer to ref. [15].

Quark mass effects for $q_T \ll m \ll Q$

First we consider the hierarchiy where the quark mass is parametrically larger than the q_T scale, $q_T \ll m$. In a first step the QCD current is matched onto the SCET current with $n_l + 1$ dynamic quark flavors at the scale $\mu \sim Q$. Since $m \ll Q$ this matching can be performed only with massless quarks, leading to the hard function with $n_l + 1$ massless flavors, $H_{ij}^{(n_l+1)}$, with the strong coupling inside it renormalized with $n_l + 1$ flavors.

In a second step at the scale $\mu \sim m$, the mass modes are integrated out and the SCET with n_l massless and one massive flavor is matched onto SCET with n_l massless flavors with the usual scaling as in the massless case. Since the soft and collinear mass modes have the same invariant mass set by the quark mass and are only separated in rapidity, there are rapidity divergences in their (unrenormalized) collinear and soft contributions. Their renormalization and the resummation of the associated logarithms can be again handled using the rapidity RG approach in refs. [12, 13], which has been explicitly carried out in ref. [16].In addition, all renormalized parameters like the strong coupling constant are matched at the mass scale from $n_l + 1$ to n_l flavors taking into account that the massive flavor is removed as a dynamic degree of freedom.

After these steps, the factorization at the low scale $\sim q_T$ proceeds as in the massless case with all operator matrix elements depending on the n_l massless flavors, which yields the factorization

theorem

$$\begin{aligned}\frac{\mathrm{d}\sigma}{\mathrm{d}q_T^2\,\mathrm{d}Q^2\,\mathrm{d}Y} = &\sum_{i,j\in\{q,\bar{q}\}} H_{ij}^{(n_l+1)}(Q,\mu)\,H_c\Big(m,\mu,\frac{\nu}{\omega_a}\Big)H_c\Big(m,\mu,\frac{\nu}{\omega_b}\Big)H_s(m,\mu,\nu)\\ &\times\int \mathrm{d}^2p_{Ta}\,\mathrm{d}^2p_{Tb}\,\mathrm{d}^2p_{Ts}\,\delta(q_T^2-|\vec{p}_{Ta}+\vec{p}_{Tb}+\vec{p}_{Ts}|^2)\,B_i^{(n_l)}\Big(\vec{p}_{Ta},x_a,\mu,\frac{\nu}{\omega_a}\Big)\\ &\times B_j^{(n_l)}\Big(\vec{p}_{Tb},x_b,\mu,\frac{\nu}{\omega_b}\Big)\,S^{(n_l)}(\vec{p}_{Ts},\mu,\nu)\,\Big[1+\mathscr{O}\Big(\frac{q_T}{Q},\frac{q_T^2}{m^2},\frac{m^2}{Q^2}\Big)\Big]\,. \end{aligned}\tag{1.4}$$

Here H_c and H_s denote the hard functions that arise from the matching at the mass scale $\mu\sim m$. Their natural rapidity scales are $\nu\sim Q$ for the collinear contributions and $\nu\sim m$ for the soft ones.

Quark mass effects for $q_T\sim m\ll Q$

If the q_T scale is of the order of the quark mass, $q_T\sim m$, the massive quark becomes a dynamic degree of freedom, which contributes to the q_T spectrum via real radiation effects. In this case, there is only a single matching at the hard scale $\mu\sim Q$ from QCD onto SCET with these common soft and collinear modes. This hard matching gives again rise to the (mass-independent) hard function $H_{ij}^{(n_l+1)}$ for n_l+1 massless flavors. The SCET operator matrix elements at the scale $\mu\sim q_T$, i.e. the beam and soft functions, now encode the effects of the massive quark. They are now renormalized with n_l+1 quark flavors and contain an explicit dependence on the quark mass. When integrating out the modes with the virtuality q_T also the massive quark is integrated out and the collinear matching functions $\mathscr{I}_{ik}$ between the beam functions and the PDFs thus also contain the effect from changing from n_l+1 to n_l flavors, i.e.

$$B_i^{(n_l+1)}\Big(\vec{p}_T,m,x,\mu,\frac{\nu}{\omega}\Big)=\sum_{k\in\{q,\bar{q},g\}}\mathscr{I}_{ik}\Big(\vec{p}_T,m,x,\mu,\frac{\nu}{\omega}\Big)\otimes_x f_k^{(n_l)}(x,\mu)\Big[1+\mathscr{O}\Big(\frac{\Lambda_{\mathrm{QCD}}^2}{m^2},\frac{\Lambda_{\mathrm{QCD}}^2}{q_T^2}\Big)\Big]\,.\tag{1.5}$$

Written out explicitly, the factorization theorem reads

$$\begin{aligned}\frac{\mathrm{d}\sigma}{\mathrm{d}q_T^2\,\mathrm{d}Q^2\,\mathrm{d}Y} = &\sum_{i,j\in\{q,\bar{q},Q,\bar{Q}\}} H_{ij}^{(n_l+1)}(Q,\mu)\int \mathrm{d}^2p_{Ta}\,\mathrm{d}^2p_{Tb}\,\mathrm{d}^2p_{Ts}\,\delta(q_T^2-|\vec{p}_{Ta}+\vec{p}_{Tb}+\vec{p}_{Ts}|^2)\\ &\times\Big[\sum_{k\in\{q,\bar{q},g\}}\mathscr{I}_{ik}\Big(\vec{p}_{Ta},m,x_a,\mu,\frac{\nu}{\omega_a}\Big)\otimes_x f_k^{(n_l)}(x_a,\mu)\Big]\\ &\times\Big[\sum_{k\in\{q,\bar{q},g\}}\mathscr{I}_{jk}\Big(\vec{p}_{Tb},m,x_b,\mu,\frac{\nu}{\omega_b}\Big)\otimes_x f_k^{(n_l)}(x_b,\mu)\Big]\\ &\times S(\vec{p}_{Ts},m,\mu,\nu)\,\Big[1+\mathscr{O}\Big(\frac{q_T}{Q},\frac{m^2}{Q^2},\frac{\Lambda_{\mathrm{QCD}}^2}{m^2},\frac{\Lambda_{\mathrm{QCD}}^2}{q_T^2}\Big)\Big]\,,\end{aligned}\tag{1.6}$$

where $i,j=Q,\bar{Q}$ denotes the massive quark flavor in the sum over flavors. While the evolution of the PDFs proceeds in n_l flavors, the μ-evolution for the hard, beam, and soft functions above the scale m is now carried out purely with n_l+1 flavors.

In this hierarchy quark mass effects enter in eq. (1.6) at $\mathscr{O}(\alpha_s^2)$ in two ways: There are secondary radiation effects appearing in the two-loop soft function $S^{(2)}$ and the flavor-diagonal beam

function matching coefficients $\mathscr{I}_{qq}^{(2)}$. In addition, there are primary mass effects arising from a massive-quark initiated hard process. For Z/γ^* production, this requires the production of the massive quarks via gluon splitting in both collinear sectors, which manifests itself in two one-loop collinear matching coefficients $\mathscr{I}_{Qg}^{(1)} \times \mathscr{I}_{\bar{Q}g}^{(1)}$. For W-boson production, primary charm quark effects enter already at $\mathscr{O}(\alpha_s)$ from a single $\mathscr{I}_{Qg}^{(1)}$ with $Q = c$. The one loop primary and two loop secondary massive quark contributions to the beam function and the massive two-loop soft function have been calculated in ref. [15].

Since the renormalization of the beam functions does not involve parton mixing, the one-loop primary mass contributions to $\mathscr{I}_{Qg}^{(1)}$ cannot give rise to rapidity divergences and associated logarithms. On the other hand, the secondary mass effects change the rapidity evolution. In particular, the beam and soft ν-anomalous dimensions become mass dependent

$$\begin{aligned}
\nu\frac{\mathrm{d}}{\mathrm{d}\nu}B_i^{(n_l+1)}\Big(\vec{p}_T,m,\mu,\frac{\nu}{\omega}\Big) &= \int \mathrm{d}^2k_T\,\gamma_{\nu,B}^{(n_l+1)}(\vec{p}_T-\vec{k}_T,m,\mu)\,B_i^{(n_l+1)}\Big(\vec{k}_T,m,\mu,\frac{\nu}{\omega}\Big)\,,\\
\nu\frac{\mathrm{d}}{\mathrm{d}\nu}S^{(n_l+1)}(\vec{p}_T,m,\mu,\nu) &= \int \mathrm{d}^2k_T\,\gamma_{\nu,S}^{(n_l+1)}(\vec{p}_T-\vec{k}_T,m,\mu)\,S^{(n_l+1)}(\vec{k}_T,m,\mu,\nu)\,.
\end{aligned} \tag{1.7}$$

where γ_ν is the rapidity anomalous dimension. We discuss the implications of the mass dependence for the rapidity evolution in sec. 2.

Quark mass effects for $m \ll q_T \ll Q$

If q_T is much larger than the mass, the fluctuations around the mass-shell take place at a different scale than the jet resolution measurement. This means that the soft modes are described by a soft function with n_l+1 massless flavors at the scale $\mu \sim q_T$. Due to the collinear sensitivity of the initial-state radiation there are still relevant collinear mass modes. Thus there are collinear modes in SCET at different invariant mass scale, which can be disentangled by a multistage matching. First, the beam functions are matched onto the PDFs with n_l massless and one massive flavor. Since this matching takes place at the scale $\mu_B \sim q_T \gg m$ this gives just the matching coefficients $\mathscr{I}_{ik}$ for n_l+1 massless flavors,

$$B_i^{(n_l+1)}\Big(\vec{p}_T,m,x,\mu,\frac{\nu}{\omega}\Big) = \sum_{k\in\{q,\bar{q},Q,\bar{Q},g\}} \mathscr{I}_{ik}^{(n_l+1)}\Big(\vec{p}_T,x,\mu,\frac{\nu}{\omega}\Big)\otimes_x f_k^{(n_l+1)}(x,m,\mu)\Big[1+\mathscr{O}\Big(\frac{m^2}{q_T^2}\Big)\Big]\,. \tag{1.8}$$

In a second step, at the mass scale $\mu_m \sim m$, the PDFs including the massive quark effects are matched onto PDFs with n_l massless quarks, and with α_s in the (n_l) flavor scheme,

$$f_i^{(n_l+1)}(x,m,\mu) = \sum_{k\in\{q,\bar{q},g\}} \mathscr{M}_{ik}(x,m,\mu)\otimes_x f_k^{(n_l)}(x,\mu)\Big[1+\mathscr{O}\Big(\frac{\Lambda_{\mathrm{QCD}}^2}{m^2}\Big)\Big]\,. \tag{1.9}$$

The PDF matching functions $\mathscr{M}_{ik}$ can be expressed in either the (n_l) or the (n_l+1) flavor scheme for α_s. The PDF matching coefficients are all known at two loops [17].

In total, the factorization theorem reads

$$\begin{aligned}\frac{\mathrm{d}\sigma}{\mathrm{d}q_T^2\,\mathrm{d}Q^2\,\mathrm{d}Y} = &\sum_{i,j\in\{q,\bar{q},Q,\bar{Q}\}} H_{ij}^{(n_l+1)}(Q,\mu)\int \mathrm{d}^2p_{Ta}\,\mathrm{d}^2p_{Tb}\,\mathrm{d}^2p_{Ts}\,\delta(q_T^2-|\vec{p}_{Ta}+\vec{p}_{Tb}+\vec{p}_{Ts}|^2)\\
&\times\left[\sum_{k\in\{q,\bar{q},Q,\bar{Q},g\}}\sum_{l\in\{q,\bar{q},g\}}\mathscr{I}_{ik}^{(n_l+1)}\Big(\vec{p}_{Ta},x_a,\mu,\frac{\nu}{\omega_a}\Big)\otimes_x\mathscr{M}_{kl}(x_a,m,\mu)\otimes_x f_l^{(n_l)}(x_a,\mu)\right]\\
&\times\left[\sum_{k\in\{q,\bar{q},Q,\bar{Q},g\}}\sum_{l\in\{q,\bar{q},g\}}\mathscr{I}_{jk}^{(n_l+1)}\Big(\vec{p}_{Tb},x_b,\mu,\frac{\nu}{\omega_b}\Big)\otimes_x\mathscr{M}_{kl}(x_b,m,\mu)\otimes_x f_l^{(n_l)}(x_b,\mu)\right]\\
&\times S^{(n_l+1)}(\vec{p}_{Ts},\mu,\nu)\left[1+\mathscr{O}\Big(\frac{q_T}{Q},\frac{m^2}{q_T^2},\frac{\Lambda_{\mathrm{QCD}}^2}{m^2}\Big)\right].\end{aligned}\tag{1.10}$$

As in (1.6), massive quark corrections can arise at $\mathscr{O}(\alpha_s^2)$ either via primary mass effects involving the product of two one-loop PDF matching corrections $\mathscr{M}_{Qg}^{(1)}$ (for Z/γ^*) generating a massive quark-antiquark pair that initiates the hard interaction, or via secondary mass effects involving one two-loop contribution $\mathscr{M}_{qq}^{(2)}$. Note that also the running of the light quark and gluon PDFs above μ_m generates an effective massive quark PDF, which for large hierarchies $m\ll q_T$ can give $\mathscr{O}(1)$ contributions.

2. Rapidity evolution

Here, we discuss the solutions of the rapidity RGEs and in particular the rapidity evolution for the mass-dependent soft function in eq. (1.7) for $q_T\sim m$, where the massive quark corrections give rise to a different running than for massless flavors. Our primary aim here is to highlight the different features with respect to the massless case, while leaving the practical implementation for future work. The rapidity evolution for the mass-mode matching functions H_s and H_c has been discussed in ref. [16].

The solution of the rapidity RGE for the soft function is substantially more involved due to its two-dimensional convolution structure on $\vec{p}_T$. The formal solution of the rapidity RGE for massless quarks is most conveniently found by Fourier transforming to impact parameter space with $b=|\vec{b}|$, where the rapidity RGE becomes multiplicative

$$\nu\frac{\mathrm{d}}{\mathrm{d}\nu}\tilde{S}^{(n_f)}(b,\mu,\nu)=\tilde{\gamma}_{\nu,S}^{(n_f)}(b,\mu)\tilde{S}^{(n_f)}(b,\mu,\nu)\,.\tag{2.1}$$

The general form of the rapidity anomalous dimension is

$$\tilde{\gamma}_{\nu,S}^{(n_f)}(b,\mu)=-4\eta_\Gamma^{(n_f)}(\mu_0(b),\mu)+\tilde{\gamma}_{\nu,S}^{(n_f)}(b,\mu_0(b))\,,\tag{2.2}$$

where the evolution function η_Γ is defined by

$$\eta_\Gamma^{(n_f)}(\mu_0,\mu)=\int_{\mu_0}^{\mu}\frac{\mathrm{d}\mu'}{\mu'}\,\Gamma_{\mathrm{cusp}}^{(n_f)}[\alpha_s^{(n_f)}(\mu')]\,.\tag{2.3}$$

The logarithms of $\ln(\mu\,b\,e^{\gamma_E}/2)$ in the second boundary term are eliminated by the canonical scale choice

$$\mu_0^{(l)}(b)=\frac{2\,e^{-\gamma_E}}{b}\,.\tag{2.4}$$

With this choice, the ν evolution of the soft function in Fourier space at any given scale μ is given by

$$\tilde{S}(b,\mu,\nu) = \tilde{S}(b,\mu,\nu_0)\exp\left[\tilde{\gamma}_{\nu,S}^{(n_f)}(b,\mu)\ln\frac{\nu}{\nu_0}\right]. \tag{2.5}$$

As is well known, the rapidity evolution kernel becomes intrinsically nonperturbative at $1/b \ll \Lambda_{\rm QCD}$ [8, 9, 10]. This nonperturbative sensitivity appears through the resummed rapidity anomalous dimension, which with the canonical scale choice in eq. (2.4) gets evaluated at $\alpha_s(1/b)$.

For the massive quark corrections in the regime $q_T \sim m$ the μ dependence of the rapidity anomalous dimension is the same as for the massless quarks, such that

$$\tilde{\gamma}_{\nu,S}^{(h)}(b,m,\mu) = 4\eta_\Gamma^{(n_l)}(\mu_0(b,m),\mu) - 4\eta_\Gamma^{(n_l+1)}(\mu_0(b,m),\mu) + \tilde{\gamma}_{\nu,S}^{(h)}(b,m,\mu_0(b,m))\,. \tag{2.6}$$

Here $\tilde{\gamma}_{\nu,S}^{(h)}$ denotes only the contributions of the massive flavor to the full anomalous dimension. The explicit mass dependence arises in the μ-independent boundary contribution, which depends on both b and m. From consistency relations we can directly infer the limiting behavior to the anomalous dimension,

$$\begin{aligned}
\tilde{\gamma}_{\nu,S}(b,m,\mu) &= \tilde{\gamma}_{\nu,S}^{(n_l+1)}(b,\mu) + \mathcal{O}(m^2b^2)\,,\\
\tilde{\gamma}_{\nu,S}(b,m,\mu) &= \tilde{\gamma}_{\nu,S}^{(n_l)}(b,\mu) + \gamma_{\nu,H_s}(m,\mu) + \mathcal{O}\Big(\frac{1}{m^2b^2}\Big)\,.
\end{aligned} \tag{2.7}$$

This means that the massive quark corrections $\tilde{\gamma}_{\nu,S}^{(h)}$ are the same as for a massless flavor in the limit $m \ll 1/b$ and are the same as the rapidity anomalous dimension of the soft mass mode function H_s in the limit $1/b \ll m$, provided one uses the (n_l+1) and (n_l)-flavor scheme for α_s, respectively. To eliminate the logarithms inside $\tilde{\gamma}_{\nu,S}^{(h)}$, the canonical scale choice $\mu_0(b,m)$ should behave like the massless case for $m \ll 1/b$ and like the choice for the mass-mode matching functions for $m \gg 1/b$,

$$\begin{aligned}
&\mu_0^{(h)}(b,m) \sim \mu_0^{(l)}(b) = \frac{2\,\mathrm{e}^{-\gamma_E}}{b} && \text{for} \quad 1/b \to \infty\,,\\
&\mu_0^{(h)}(b,m) \sim m && \text{for} \quad 1/b \to 0\,.
\end{aligned} \tag{2.8}$$

Since $\mu_0^{(h)}(b,m)$ freezes out naturally at the perturbative mass scale for $1/b \to 0$, the nonperturbative sensitivity in the ν evolution gets regulated by the quark mass for the massive quark contributions. A convenient choice to eliminate any large terms in both limits is

$$\mu_0^{(h)}(b,m) = m\,e^{K_0(bm)}\,, \tag{2.9}$$

where K_0 denotes the modified Bessel function of the second kind. The behavior of this choice as a function of b compared to the massless result is shown in fig. 2.

The full secondary massive quark corrections at $\mathcal{O}(\alpha_s^2)$ to the rapidity anomalous dimension of the soft function in Fourier space read

$$\begin{aligned}
\tilde{\gamma}_{\nu,S}^{(h)}(b,m,\mu) = \Big(\frac{\alpha_s^{(n_l+1)}(\mu)}{4\pi}\Big)^2 C_F T_F \Big\{ &-\frac{32}{3}L_bL_m - \frac{16}{3}L_m^2 - \frac{160}{9}L_m - \frac{448}{27}\\
&+ \frac{8\sqrt{\pi}}{3}\Big[2\,G_{1,3}^{3,0}\Big(\begin{smallmatrix}\frac{3}{2}\\ 0,0,0\end{smallmatrix}\Big|\,m^2b^2\Big) + G_{1,3}^{3,0}\Big(\begin{smallmatrix}\frac{5}{2}\\ 0,0,1\end{smallmatrix}\Big|\,m^2b^2\Big)\Big]\Big\}\,,
\end{aligned} \tag{2.10}$$

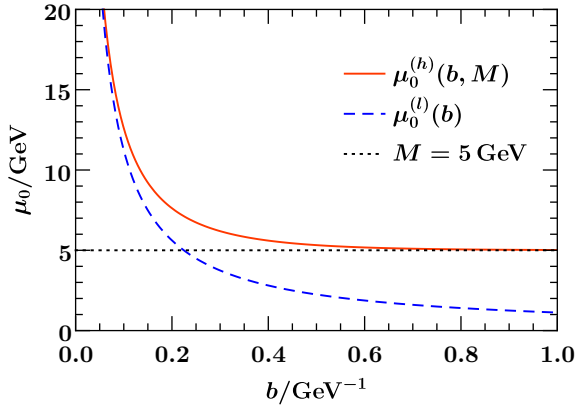

Figure 2: The canonical scales $\mu_0^{(h)}(b,M)$ for the massive case (red, solid) and $\mu_0^{(l)}(b) = \mu_0(b,M=0)$ for the massless case (blue, dashed) with $M = 5$ GeV.

where G denotes a Meijer G function and $L_b \equiv \ln \frac{b^2\mu^2 e^{2\gamma_E}}{4}$ and $L_m \equiv \ln \frac{m^2}{\mu^2}$.

This result has the limiting behavior

$$\begin{aligned}
&\tilde{\gamma}_{\nu,S}^{(h)}(b,m,\mu) = \left(\frac{\alpha_s^{(n_l+1)}(\mu)}{4\pi}\right)^2 C_F T_F \left(\frac{16}{3}L_b^2 + \frac{160}{9}L_b + \frac{448}{27}\right) + \mathcal{O}(m^2b^2)\,,\\
&\tilde{\gamma}_{\nu,S}^{(h)}(b,m,\mu) - \left(\frac{\alpha_s^{(n_l)}(\mu)}{4\pi}\right)\frac{4}{3}L_m\tilde{\gamma}_{\nu,S}^{(1)}(b,\mu)\\
&\qquad = \left(\frac{\alpha_s^{(n_l+1)}(\mu)}{4\pi}\right)^2 C_F T_F \left(-\frac{16}{3}L_m^2 - \frac{160}{9}L_m - \frac{448}{27}\right) + \mathcal{O}\left(\frac{1}{m^2b^2}\right),
\end{aligned} \tag{2.11}$$

where $\tilde{\gamma}_{\nu,S}^{(1)}$ is the one loop anomalous dimension. This term arises when changing the strong coupling from the n_l+1 to the n_l flavor scheme, which is necessary to get both limits correctly. To minimize the logarithms for any regime one should thus adopt a canonical scale choice that satisfies eq. (2.8), as for example in eq. (2.9).

3. Outlook: Phenomenological impact for Drell-Yan

An accurate description of the q_T spectrum is also a key ingredient for a precise measurement of the W-boson mass at the LHC, which requires a thorough understanding of the W-boson and Z-boson spectra and in particular their ratio [18, 19, 20, 21]. The associated uncertainties are one of the dominant theoretical uncertainties in the recent m_W determination by the ATLAS collaboration [22]. Our results can be applied to properly take into account bottom quark mass effects for the Drell-Yan q_T spectrum at NNLL$'$. While a full resummation analysis is beyond the scope of this paper, we can estimate the potential size of the quark-mass effects by looking at the fixed-order q_T spectrum.

In fig. 3, we show separately the contributions from primary and secondary massive quarks to the cross section at $\mathcal{O}(\alpha_s^2)$, normalized to the $\mathcal{O}(\alpha_s)$ spectrum $\mathrm{d}\sigma^{(1)}$ including all flavors (treating the charm as a massless flavor). We utilize the MMHT2014 NNLO PDFs [23] and evaluate the

contributions for $\mu = m_b = 4.8$ GeV, $Q = m_Z$, $Y = 0$, and $E_{\text{cm}} = 13$ TeV. Note that the secondary mass contributions at $\mathcal{O}(\alpha_s^2)$ are explicitly μ-dependent and scheme-dependent, the nonsingular mass correction, i.e. the difference between the full massive result for $\mu \sim m_b$ and the massless limit (encoded partially in a massive PDF), is μ independent at this order. As can be seen, the relative contribution of the $b\bar{b}$-initiated channel grows with larger q_T, while the impact of the secondary contributions including the full mass dependence is at the sub-percent level throughout the spectrum. As expected, the nonsingular mass corrections are very small for $m_b \ll q_T$, but can reach the order of percent for $q_T \sim m_b$, which roughly corresponds to the peak region of the distribution where the cross section is largest.

The same can also be seen in fig. 4, where we show the mass nonsingular corrections to the massless limit for primary and secondary contributions as well as their sum. They are shown for $\mu = m_b$ on the left and for $\mu = q_T$ on the right. We see that these corrections are (at fixed order) indeed only weakly dependent on the value of μ (for $q_T \gtrsim 2$ GeV). All in all, the bottom quark mass can have a relevant effect for high precision predictions of the q_T-spectrum at the order of percent around the peak of the distribution (~ 5 GeV). Below the peak of the distribution the fixed-order result is of course not expected to give a reliable quantitative result, and furthermore nonperturbative corrections become important in this regime. Nevertheless, we expect the qualitative features like the sign and order of magnitude of the mass effects to provide an indication for the behaviour of the full resummed result.

For W production sizable corrections from bottom quark effects arise only through secondary contributions (due to the strong CKM suppression of the primary contributions), which have a similar impact as for Z-production. On the other hand, charm-initiated production plays an important role and enters already at $\mathcal{O}(\alpha_s)$. Estimating the nonsingular mass corrections for $q_T \sim m_c$ is more subtle, since higher-order corrections in the strong coupling and nonperturbative effects are likely to dominate the effect from the known beam function at $\mathcal{O}(\alpha_s)$ at these low scales. Thus, we do not attempt to determine their characteristic size here and leave this to future work. An analysis based on the leading-order matrix element and its potential impact on the determination of m_W can be found in ref. [24].

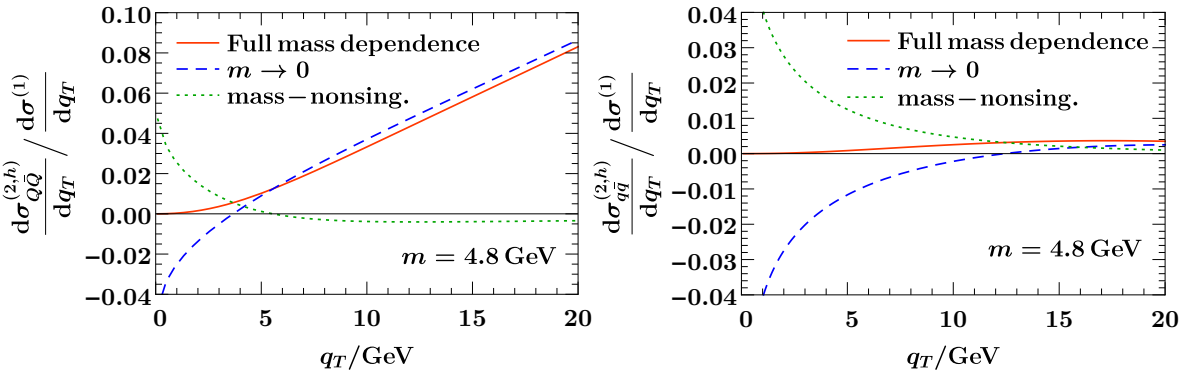

Figure 3: Primary (left panel) and secondary (right panel) massive bottom quark contributions for the Z-boson q_T spectrum at fixed $\mathcal{O}(\alpha_s^2 T_F^2)$ and $\mathcal{O}(\alpha_s^2 C_F T_F)$, respectively. The results are given relative to the full $\mathcal{O}(\alpha_s)$ result including all flavors.

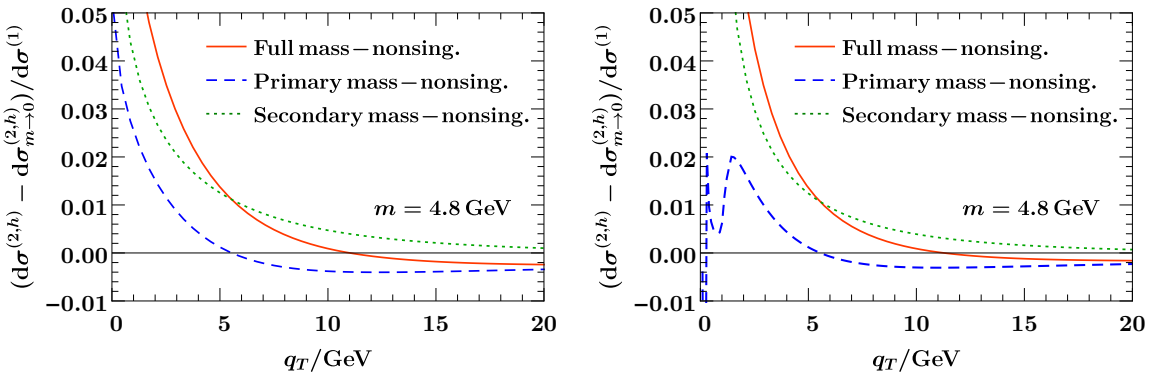

Figure 4: Different types of mass nonsingular corrections for Z-boson production at $\mu = m_b$ (left panel) and $\mu = q_T$ (right panel).

References

[1] J. C. Collins and D. E. Soper, *Parton Distribution and Decay Functions*, *Nucl. Phys.* **B194** (1982) 445–492.

[2] S. Fleming, A. K. Leibovich, and T. Mehen, *Resummation of Large Endpoint Corrections to Color-Octet J/ψ Photoproduction*, *Phys. Rev.* **D74** (2006) 114004, [hep-ph/0607121].

[3] I. W. Stewart, F. J. Tackmann, and W. J. Waalewijn, *Factorization at the LHC: From PDFs to Initial State Jets*, *Phys.Rev.* **D81** (2010) 094035, [arXiv:0910.0467].

[4] S. Catani, L. Cieri, D. de Florian, G. Ferrera, and M. Grazzini, *Vector boson production at hadron colliders: hard-collinear coefficients at the NNLO*, *Eur. Phys. J.* **C72** (2012) 2195, [arXiv:1209.0158].

[5] T. Gehrmann, T. Lubbert, and L. L. Yang, *Transverse parton distribution functions at next-to-next-to-leading order: the quark-to-quark case*, *Phys. Rev. Lett.* **109** (2012) 242003, [arXiv:1209.0682].

[6] T. Gehrmann, T. Luebbert, and L. L. Yang, *Calculation of the transverse parton distribution functions at next-to-next-to-leading order*, *JHEP* **06** (2014) 155, [arXiv:1403.6451].

[7] T. Lübbert, J. Oredsson, and M. Stahlhofen, *Rapidity renormalized TMD soft and beam functions at two loops*, *JHEP* **03** (2016) 168, [arXiv:1602.01829].

[8] J. C. Collins and D. E. Soper, *Back-To-Back Jets in QCD*, *Nucl. Phys.* **B193** (1981) 381. [Erratum: Nucl. Phys.B213,545(1983)].

[9] J. C. Collins and D. E. Soper, *Back-To-Back Jets: Fourier Transform from B to K-Transverse*, *Nucl. Phys.* **B197** (1982) 446–476.

[10] J. C. Collins, D. E. Soper, and G. F. Sterman, *Transverse Momentum Distribution in Drell-Yan Pair and W and Z Boson Production*, *Nucl. Phys.* **B250** (1985) 199.

[11] T. Becher and M. Neubert, *Drell-Yan production at small q_T, transverse parton distributions and the collinear anomaly*, *Eur.Phys.J.* **C71** (2011) 1665, [arXiv:1007.4005].

[12] J.-Y. Chiu, A. Jain, D. Neill, and I. Z. Rothstein, *The Rapidity Renormalization Group*, *Phys.Rev.Lett.* **108** (2012) 151601, [arXiv:1104.0881].

[13] J.-Y. Chiu, A. Jain, D. Neill, and I. Z. Rothstein, *A Formalism for the Systematic Treatment of Rapidity Logarithms in Quantum Field Theory*, *JHEP* **1205** (2012) 084, [arXiv:1202.0814].

[14] M. G. Echevarria, A. Idilbi, and I. Scimemi, *Factorization Theorem For Drell-Yan At Low q_T And Transverse Momentum Distributions On-The-Light-Cone*, *JHEP* **07** (2012) 002, [arXiv:1111.4996].

[15] P. Pietrulewicz, D. Samitz, A. Spiering, and F. J. Tackmann, *Factorization and Resummation for Massive Quark Effects in Exclusive Drell-Yan*, *JHEP* **08** (2017) 114, [arXiv:1703.09702].

[16] A. H. Hoang, A. Pathak, P. Pietrulewicz, and I. W. Stewart, *Hard Matching for Boosted Tops at Two Loops*, *JHEP* **12** (2015) 059, [arXiv:1508.04137].

[17] M. Buza, Y. Matiounine, J. Smith, and W. L. van Neerven, *Charm electroproduction viewed in the variable flavor number scheme versus fixed order perturbation theory*, *Eur. Phys. J.* **C1** (1998) 301–320, [hep-ph/9612398].

[18] V. Buge, C. Jung, G. Quast, A. Ghezzi, M. Malberti, and T. Tabarelli de Fatis, *Prospects for the precision measurement of the W mass with the CMS detector at the LHC*, *J. Phys.* **G34** (2007) N193–N220.

[19] **ATLAS** Collaboration, N. Besson, M. Boonekamp, E. Klinkby, S. Mehlhase, and T. Petersen, *Re-evaluation of the LHC potential for the measurement of Mw*, *Eur. Phys. J.* **C57** (2008) 627–651, [arXiv:0805.2093].

[20] **CMS** Collaboration, *W-like measurement of the Z boson mass using dimuon events collected in pp collisions at $\sqrt{s} = 7$ TeV*, . CMS-PAS-SMP-14-007 (2016).

[21] **ATLAS** Collaboration, G. Aad *et al.*, *Studies of theoretical uncertainties on the measurement of the mass of the W boson at the LHC*, . ATL-PHYS-PUB-2014-015.

[22] **ATLAS** Collaboration, M. Aaboud *et al.*, *Measurement of the W-boson mass in pp collisions at $\sqrt{s} = 7$ TeV with the ATLAS detector*, arXiv:1701.07240.

[23] L. A. Harland-Lang, A. D. Martin, P. Motylinski, and R. S. Thorne, *Parton distributions in the LHC era: MMHT 2014 PDFs*, *Eur. Phys. J.* **C75** (2015), no. 5 204, [arXiv:1412.3989].

[24] S. Berge, P. M. Nadolsky, and F. I. Olness, *Heavy-flavor effects in soft gluon resummation for electroweak boson production at hadron colliders*, *Phys. Rev.* **D73** (2006) 013002, [hep-ph/0509023].

PoS(RADCOR2017)053